

Phenomenological theory of kinetic friction for the solid lubricant film

O M Braun

Institute of Physics, National Academy of Sciences of Ukraine, 03028 Kiev, Ukraine

E-mail: obraun@iop.kiev.ua

Received 15 April 2008

Accepted for publication 19 May 2008

Published 30 June 2008

Online at stacks.iop.org/PhysScr/78/015802

Abstract

Molecular dynamics based on the Langevin equations with the coordinate- and velocity-dependent damping coefficients is used to investigate the friction properties of a ‘hard’ lubricant film confined between two solids, when the lubricant remains in the solid state during sliding. The dependence of the friction force on the temperature and sliding velocity in the smooth sliding regime is studied in detail for all three states of the lubricant: a lubricant with a crystalline structure, when the system exhibits a very low friction (superlubricity), an amorphous lubricant structure, which results in a high friction, and the liquid state of the lubricant film at high temperatures or velocities. A phenomenological theory of the kinetic friction is developed, which allows us to explain the simulation results and predict a variation of the friction properties with model parameters analytically.

PACS numbers: 81.40.Pq, 46.55.+d

(Some figures in this article are in colour only in the electronic version.)

1. Introduction

The problem of friction is one of the oldest physical problems and, despite its great practical importance, is still not fully understood [1]. Molecular dynamics (MD) simulation of confined driven systems, which allows us to calculate the kinetic friction at huge sliding velocities ($> 1 \text{ m s}^{-1}$), has played an increasingly significant role in tribology in the last decade [2, 3]. The first systematic MD study of sliding for two substrates separated by a thin lubricant film, based on the Langevin equations, was conducted by Thompson and Robbins [4]. These authors considered a typical case of a ‘soft’ lubricant, when the amplitude of the interatomic interaction within the lubricant, V_{ll} , is weaker than the lubricant–substrate interaction, V_{sl} . It was shown that when the top substrate is driven at a low velocity through an attached spring, the system exhibits stick–slip motion due to the melting/freezing mechanism: the lubricant film melts at the onset of sliding and solidifies again at stick. These results were later confirmed in a number of simulations and are in agreement with many experimental studies (see e.g. [1–3] and references therein).

Despite the great progress in MD simulation of friction achieved in recent years, it still remains on an empirical level. The MD simulation, being quite time consuming, provides the

value of friction only for a given set of model parameters and may hardly lead to an understanding of the general trends or laws, e.g. the dependence of friction on temperature, sliding velocity, shape of lubricant molecules, parameters of the interaction between the lubricant and substrates, etc. The reason lies in the complexity of processes in these highly nonequilibrium systems. The kinetic friction force F_k appears due to energy flow from the sliding interface into the bulk of substrates, which finally is to be converted to heat. The energy losses emerge because of the creation of phonons and, with a lower rate, the electron–hole pairs in the case of metal substrates. The rate of phonon creation depends on many factors, such as the density of phonon states, positions and velocities of the lubricant atoms relative to the surfaces, which in turn depend on the sliding velocity, the heating of the interface due to sliding, etc.

In this work, we present the first attempt to describe this problem analytically. We made a detailed MD simulation of the sliding interface and then, extracting the necessary parameters from the simulation, constructed a phenomenological theory of kinetic friction. In the result, we obtained the dependence of the friction force on system characteristics, which should allow us to find the value of kinetic friction in the general case, i.e. to predict the value of F_k and its variation with sliding conditions without making large-scale

MD simulations. Here, we consider a simpler problem of kinetic friction, when the sliding velocity is huge, and the system is in the well-defined steady-state regime.

In this work, we consider the case of a ‘hard’ lubricant, when the amplitude of interaction between the lubricant atoms is larger than the lubricant–substrate interaction ($V_{sl} < V_{ll}$) and the lubricant remains in a solid state during sliding [5]. The use of solid lubricants is a very promising way to decrease friction, especially in nano- and microdevices. Well-known examples include layered materials such as graphite, MoS₂ and Ti₃SiC₂. The solid lubricants may provide very low friction due to incommensurability of the crystalline surfaces [2, 3, 6–8]. However, if the ideal crystalline structure of the lubricant is destroyed, e.g. due to sliding, the lubricant takes an amorphous structure characterized by quite high friction. Therefore, understanding the processes that take place in a thin solid film confined between two solid surfaces in relative motion is of great importance in designing the best lubricants.

There are only a few studies of the hard lubricant. Thompson and Robbins [4] studied the hard lubricant system, $V_{sl} \leq 0.4V_{ll}$, for a film thickness of > 10 molecular diameters at a relatively high temperature, $k_B T = 1.1V_{ll}$, which is 30% higher than the bulk melting temperature of the lubricant. It was shown that during slips the lubricant slides with respect to the substrates, i.e. there is a nonzero jump, Δv_x , of the velocity between the $z = 0$ plane (the substrate’s surface) and the $z = z_1$ plane which corresponds to the first lubricant layer (x is the sliding direction and z is perpendicular to the surfaces). The amplitude of the jump Δv_x decreases when the ratio V_{sl}/V_{ll} increases, i.e. the jump would disappear for the soft lubricant system. The case of an amorphous lubricant has also been studied by Thompson *et al* [12]. It was observed that when the lubricant is frozen in a glassy state, all the shear occurs at the lubricant/substrate interface.

In the present work, we present the results for a five-layer lubricant film only (some results for other cases may be found in [3, 5]; a detailed MD simulation of kinetic friction for submonolayer lubricant films has been presented by He and Robbins [10]). The paper consists of two parts: section 2 is devoted to MD simulation, whereas section 3 describes the phenomenological theory developed to explain the simulation results analytically.

In the simulation, we used the method developed earlier in [5]. It is based on Langevin equations with the coordinate- and velocity-dependent damping coefficient (see section 2.1), which mimics a realistic situation in the nonequilibrium driven system. The results of simulation are presented in section 2.2. Depending on the driving velocity and temperature, the system exhibits three types of sliding: the perfect sliding, the sliding with the ‘amorphous’ lubricant and the liquid sliding (LS). The perfect sliding regime (also known as ‘superlubricity’ or ‘structural lubricity’) is characterized by very low friction. It is observed when the lubricant has a crystalline structure, so that the sliding occurs at the incommensurate lubricant/substrate interface. The second (‘amorphous’) regime emerges when, after melting because of sliding, the lubricant freezes at stick in a metastable configuration. The friction coefficient in this case is high. Finally, at a high driving velocity and/or temperature,

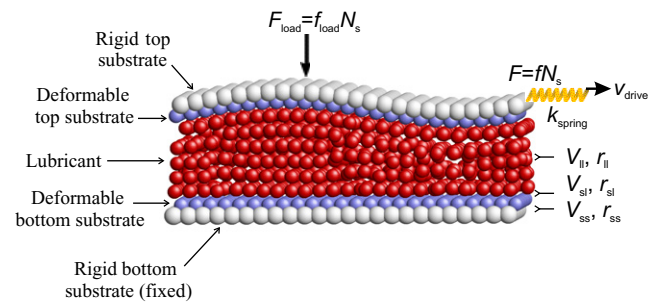


Figure 1. The model used in the MD simulation of friction. Each substrate consists of two layers: the rigid layer and the deformable substrate layer which is in contact with the lubricant. The lubricant atoms fill the space between the substrates. The atoms of the rigid layer of the bottom substrate are fixed, whereas the rigid layer of the top substrate can move due to applied forces.

the lubricant film is melted, and the LS regime with an intermediate value of the friction coefficient takes place. For all three regimes, we studied in detail the dependence of the friction force on the driving velocity and temperature.

In section 3, we develop the phenomenological theory, which allows us to explain the simulation results of section 2 as well as to predict the friction properties of similar systems without (or before) making MD simulations. The theory is based on energy balance arguments (see section 3.1): the energy pumped into the system due to driving must be dissipated within the system and finally taken away from it. Therefore, the kinetic friction is determined first of all by the rate of energy flux from lubricant atoms that move relative the surfaces, to the substrates. However, one has to take into account two more issues: firstly, the lubricant is always heated due to driving (see section 3.3), and secondly, the lubricant structure depends on the sliding steady state (section 3.2). Thus, the kinetic friction force is determined by a rather delicate balance of all these factors. The theory is then applied to the simulation results of section 2: to the perfect sliding regime (section 3.4), to the case of a solid lubricant with an ‘amorphous’ structure (section 3.5) and to the LS regime (section 3.6).

Finally, section 4 concludes the paper with a short discussion of the results.

2. Simulation

2.1. Model

The model was described in the papers [3, 5] and therefore we only briefly discuss here its main features. Using MD, we study a few-atomic-layer film between two (top and bottom) substrates (see figure 1). Each substrate is made of two layers. One is fully rigid with the square symmetry, while the dynamics of the atoms belonging to the layer in contact with the lubricant is included in the study. The rigid part of the bottom substrate is fixed at $x = y = z = 0$, whereas the rigid layer of the top substrate is mobile in the three directions of space x , y and z .

All the atoms interact with the Lennard–Jones potentials $V(r) = V_{\alpha\alpha'} [(r_{\alpha\alpha'}/r)^{12} - 2(r_{\alpha\alpha'}/r)^6]$, where $\alpha = s$ or l for the substrate or lubricant atoms, respectively. The parameters $V_{\alpha\alpha'}$ and $r_{\alpha\alpha'}$ depend on the type of atoms and the usual

truncation to $r \geq r^* = 1.49 r_{\parallel}$ is used. Between two substrate atoms, we use $V_{ss} = 3$ and the equilibrium distance $r_{ss} = 3$. The interaction between the substrate and the lubricant is much weaker with $V_{sl} = 1/3$. For the lubricant itself, we consider the case of a hard lubricant with $V_{ll} = 1$ (although the lubricant is less rigid than the substrates) and the equilibrium distance $r_{ll} = 4.14$, which is ‘incommensurate’ with the equilibrium distance in the substrate. The parameter r_{sl} characterizing the interaction between the substrate and the lubricant is $r_{sl} = 0.5(r_{ss} + r_{ll})$. The atomic masses are $m_1 = m_s = 1$. The two substrates are pressed together by a loading force f_{load} per atom (typically we used the value $f_{\text{load}} = 0.1$). All the parameters are given in dimensionless (natural) units.

It is useful to couple the natural units with the Système International (SI). The basic parameters that are unchanged in the simulations are: the amplitude of interaction within the substrates ($V_{ss} = 3$), which sets the energy parameter, the substrate lattice constant ($a_s = 3$) that sets the length scale, and the mass of the lubricant atoms ($m_1 = 1$) as the mass parameter. Let a real system be characterized by the amplitude of interaction in the substrates \tilde{V}_{ss} measured in eV, by the substrate lattice constant \tilde{a}_s measured in angström, and by the mass of lubricant atoms \tilde{m}_1 measured in proton masses m_p . If we introduce the following coefficients: $v_e = \tilde{V}_{ss}/V_{ss}$, $v_r = \tilde{a}_s/a_s$ and $v_m = \tilde{m}_1/(100 m_1)$, then $v_e \sim v_r \sim v_m \sim 1$ for a typical system, and we have for the unit of length $1 \text{ m} = 10^{10} v_r^{-1} \text{ n.u.}$, for the unit of mass $1 \text{ kg} = 6 \times 10^{24} v_m^{-1} \text{ n.u.}$, for the unit of energy $1 \text{ J} = 6.25 \times 10^{18} v_e^{-1} \text{ n.u.}$, for the unit of force $1 \text{ N} = 6.25 \times 10^8 (v_r/v_e) \text{ n.u.}$, for the unit of pressure $1 \text{ Pa} = 6.25 \times 10^{-12} (v_r^3/v_e) \text{ n.u.}$, for the unit of time $1 \text{ s} = 0.98 \times 10^{13} (v_e/v_m v_r^2)^{1/2} \text{ n.u.}$ and for the unit of velocity $1 \text{ m s}^{-1} = 1.02 \times 10^{-3} (v_m/v_e)^{1/2} \text{ n.u.}$

The main difference between our technique and other simulations of confined systems [2, 4, 9, 10] lies in the coupling with the heat bath, i.e. the part of the material that is not explicitly included in the simulation. We use the Langevin dynamics with a coordinate- and velocity-dependent damping coefficient $\eta(z, v)$, which has been designed to mimic a realistic situation, and was presented in detail in [3, 5]. In a driven system, the energy pumped into the system must then be removed from it. However, the energy loss comes from the degrees of freedom that are not included in the calculation, i.e. the transfer of energy to the bulk of the substrate. Therefore, the damping must depend on the distance z between an atom and the substrate. Moreover, the efficiency of the transfer should depend on the velocity v of the atom because it affects the frequencies of the motions that it excites within the substrates. In our model, the damping is written as $\eta(z, v) = \eta_1(z) \eta_2(v)$. The first factor

$$\eta_1(z) = 1 - \tanh[(z - z^*)/z^*] \quad (1)$$

(with $z^* = 2.12$ as the model parameter) describes the exponential decrease of the damping rate when an atom is shifted away from the substrate. The second factor $\eta_2(v)$ describes the velocity-dependent excitation of phonons in the substrate, which was taken in the form

$$\eta_2(v) = \eta_{\min} + 16 \omega_m \left[\frac{\omega(v)}{\omega_m} \right]^4 \left(1 - \left[\frac{\omega(v)}{\omega_m} \right]^2 \right)^{3/2}, \quad (2)$$

where the minimal contribution η_{\min} comes from the electron–hole and multi-phonon damping mechanisms (we used $\eta_{\min} = 0.01 \omega_s$ in the simulation, where $\omega_s \approx 4.9$ is the characteristic substrate frequency), while the second term in the rhs of (2) describes the one-phonon damping, ω_m is the cutoff (Debye) frequency ($\omega_m = 15$ in the simulation) and $\omega(v) = 2\pi v/a_s$ is the ‘washboard’ frequency [3, 5]. A method of solving the Langevin equations with the coordinate- and velocity-dependent damping coefficient may be found in [3, 11, 12].

The initial configuration of the lubricant was prepared as a set of $N_l = 5$ closely packed atomic layers. Most of the simulations have been performed with 80 or 160 atoms in each lubricant layer. The system was heated up to a temperature lower than the melting temperature and then relaxed during the adiabatic decrease of T . In this way we obtained the ground-state (GS) configuration, which corresponds to the minimum of the potential energy of the system. Such a configuration has an ‘ideal’ crystalline structure and provides the lowest friction as described below. In another set of simulation runs, the initial configuration was prepared with the help of annealing of the GS configuration, i.e. by the adiabatic increase of the temperature to $T \sim 0.6$ (which is above the melting temperature T_{melt}) and then its decrease back to zero. In these cases, the initial configuration corresponds to a metastable (‘amorphous’) state.

In the model with periodic boundary conditions in the x - and y -directions that we use here, the results may be sensitive to the total number of lubricant atoms N . If N does not match exactly the number of atoms in closely packed layers, then extra atoms or vacancies will produce structural defects, especially in small systems accessible in simulations. To reduce uncertainties due to this difficulty, we also used a geometry with a curved top substrate [13] (see figure 1), when the z -coordinate of the rigid layer of the top substrate varies along the x -direction by $\Delta z = 0.5 r_{sl} (1 - \cos 2\pi x/L)$, where L is the x -size of the system. Such a geometry is also closer to real situations, where the surfaces are often rough.

In simulations, we used two different algorithms. In the constant-force algorithm, the driving force f is applied directly to the rigid layer of the top substrate. The force is increased adiabatically to find the static friction force f_s and investigate the system dynamics during sliding. Then f decreases adiabatically until the sliding stops. In the algorithm with an attached spring, a spring is attached to the rigid top layer, and the spring’s end is driven with a constant velocity v_s . In this case, the spring constant k_s models the elasticity of the top substrate.

2.2. Results

2.2.1. The perfect sliding. For the GS initial configuration at $T = 0$, the situation corresponds to the ideal (perfect) sliding, when the lubricant film slides as a whole with respect to the substrates, and its behaviour may approximately be described by the ‘universal’ dependence [3, 5]. The kinetic friction in this case is due to excitation of phonons in the lubricant and in the substrates. The effective friction is high when the washboard frequency $\omega_{\text{wash}} = 2\pi v_{\text{lub}}/a_s$ lies inside the substrate phonon spectrum. For the chosen model parameters,

the phonon spectrum of the lubricant has a maximum at $\omega \approx 3$. As a result, the phonon damping reaches its maximum at $v_{\text{top}} \sim 1$. At low velocities $v \ll 1$, the kinetic friction strongly decreases with velocity, $f_k \propto v^4$, because of the dependence of the coefficient η_2 on v (see (2)). The perfect-sliding regime provides the minimal kinetic friction (superlubricity). The lubricant is heated due to sliding, but its state does not correspond to thermal equilibrium, $T_z > T_x > T_y$ (lubricant temperature is defined as the average kinetic energy; for details see [5]). At low velocities, $v \ll 1$, the temperature is not uniformly distributed over the lubricant film; the boundary layers that are in moving contact with the substrates have a slightly higher temperature than those in the middle of the lubricant [5]. However, at higher velocities, $v_{\text{top}} > 1$, the lubricant temperature is approximately uniform across the lubricant. The hysteresis of $v_{\text{top}}(f)$, when the dc force f increases above f_s and then decreases back to zero, exists due to inertia effects. When the force f decreases below the backward threshold $f = f_b \ll f_s$, the velocity drops from a finite value $v = v_b \sim 0.03\text{--}0.1$ to zero, and the system comes back to the crystalline configuration.

The simulation with the attached spring algorithm demonstrates the following sequence of transitions with the increasing of driving velocity: stick–slip motion at low velocities \rightarrow irregular (chaotic) motion at an intermediate velocity \rightarrow smooth motion corresponding to the perfect sliding at high velocities [3]. In the stick–slip regime, the spring force f grows linearly with time up to f_s , at which moment the top substrate begins to move with the velocity $v = v_{\text{top}}(f_s) \sim 0.1$. After that, the spring contracts and f drops down to the backward threshold value f_b when the motion stops; the whole cycle is then repeated. The lubricant temperature increases during the slip but remains much lower than the melting temperature, $T_{\text{lub}} \ll T_{\text{melt}} = 0.44$ (see [14]). The lubricant thickness also increases just at the onset of sliding, but the variation is very small, $< 1\%$. The transition from stick–slip to smooth sliding is smooth and takes place in an interval of velocities around a ‘critical’ velocity $v_c \sim v_b \sim 0.03$.

Note that the dependences of the friction force on the spring velocity in the smooth-sliding regime agree with the $v_{\text{top}}(f)$ dependences obtained with the help of the constant-force algorithm. We emphasize that during smooth sliding the kinetic frictional force is extremely small, $f_k \sim 10^{-4}\text{--}10^{-3}$, and strongly increases with the driving velocity. In addition, we did not observe any hysteresis in system behaviour when v_s increases above v_c and then decreases back to smaller values. Moreover, the static friction force in the stick–slip regime is approximately constant and does not depend on the driving velocity, i.e. we have not observed any ‘aging’ of the lubricant film (contrary to the soft lubricant system [3]). Thus, we conclude that the transition from stick–slip to smooth sliding is governed by the inertia mechanism.

2.2.2. ‘Amorphous’ lubricant. When the temperature increases above T_{melt} and then decreases back to zero, the lubricant film freezes in a metastable state and takes a configuration of $N_1 + 1$ layers with defects (dislocations) [5]. We call such a configuration ‘amorphous’ to distinguish it

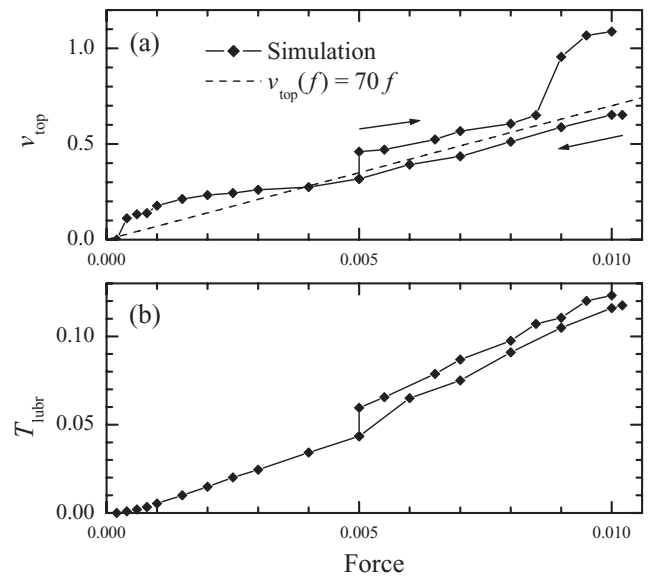


Figure 2. The velocity of the top substrate (a) and the lubricant temperature (b) as a function of the applied dc force for the ‘amorphous’ lubricant with flat surfaces.

from the previous case of crystalline lubricant structure. The static friction force is not uniquely defined in the ‘amorphous’ lubricant case, because f_s depends on the structure of the given metastable configuration. If one uses the constant-force algorithm in this case, the system has typically no steady state for $f > f_s$, because the velocity at the onset of sliding grows fast, and the system cannot dissipate the energy pumped into it due to driving. The lubricant’s thickness and temperature increase with time, whereas the external damping coefficient decreases according to (1) and (2), and finally, the system becomes unstable, $v_{\text{top}} \rightarrow \infty$. However, if one decreases the dc force, the solid-sliding regime is again observed, when the lubricant film slides as a whole. A typical example is shown in figure 2. The dependence $v_{\text{top}}(f)$ is not uniquely defined as well, because it depends on the particular metastable configuration. Moreover, during sliding the lubricant may reorder, which results in the increase of v_{top} (i.e. the decrease of kinetic friction). At low driving velocities, the sliding is typically asymmetric, the lubricant film sticks to either the bottom or the top substrate and the sliding takes place at a single lubricant/substrate interface only. The lubricant is heated due to sliding (now $T_x \approx T_y \approx T_z$), but its temperature remains below the melting temperature, so that the lubricant keeps the six-layer configuration with defects. Note that the mobility of the frozen lubricant is much smaller than that of the ideal lubricant film for the same interval of forces.

For the curved top substrate, the $T = 0$ annealed configuration has five layers in the narrow region and six layers in the wide region as shown in figure 3. The dependences obtained with the constant-force algorithm for this case are shown in figure 4. The lubricant moves as a whole together with the top (curved) substrate for forces $f < 0.03$, while at higher forces the lubricant is melted.

2.2.3. Role of the temperature. The simulation results obtained with the constant-force algorithm at different temperatures of the substrate are summarized in figure 5.

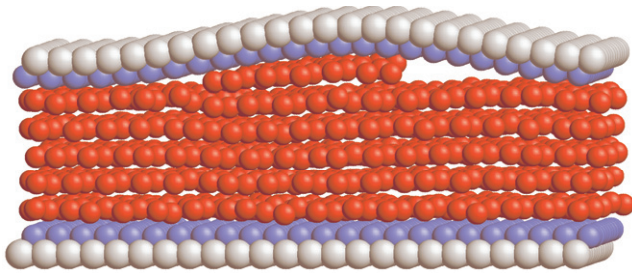


Figure 3. The configuration of the lubricant film with the curved top substrate at $f = 0.02$ (the figure was produced with RasTop software [15]).

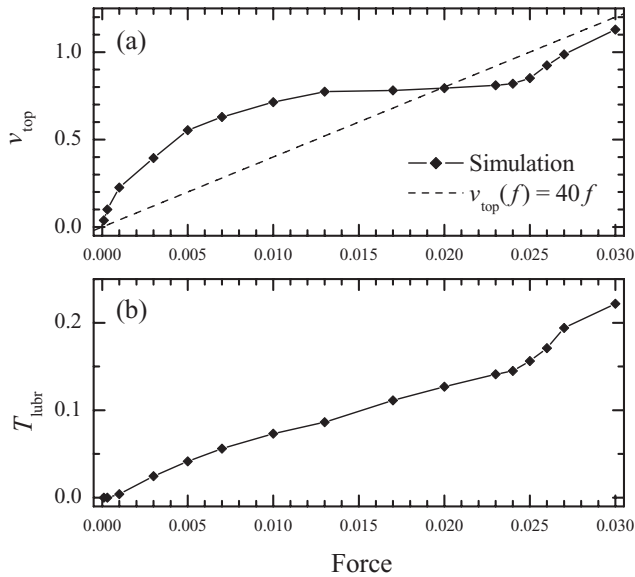


Figure 4. The velocity of the top substrate (a) and the lubricant temperature (b) as a function of the dc force for the curved geometry.

When the applied force is below the static friction force, $f < f_s$, the velocity is zero in the $T = 0$ case. If now one increases the temperature, the velocity v_{top} will increase with T due to thermally activated (creep) motion. However, if the system is already in the perfect-sliding regime (even if $f < f_s$ but $f > f_b$), then v_{top} decreases when T grows up to the melting temperature. The substrate temperature has almost no effect until it is lower than T_{eff} (the heating of the lubricant due to sliding), so that at high driving velocities the role of T is negligible. With the further increase of T , when the lubricant melts, v_{top} increases, but it remains lower than that of the $T = 0$ perfect-sliding steady state. In the molten state, the distribution of atomic velocities across the lubricant, $v_x(z)$, exhibits an approximately constant gradient as shown in figure 6.

If the lubricant film is annealed, then it freezes in a metastable configuration [14]. The force–velocity characteristics for the ‘amorphous’ lubricant at different temperatures are presented in figure 7, where T was increased starting from the frozen state. One can see that the mobility of the frozen lubricant is much lower than that of the perfect solid lubricant. Again, the velocity decreases when T grows until the lubricant melts; after that v_{top} increases with T .

Finally, the role of temperature for the case of the curved top substrate is qualitatively similar to that of the flat system.

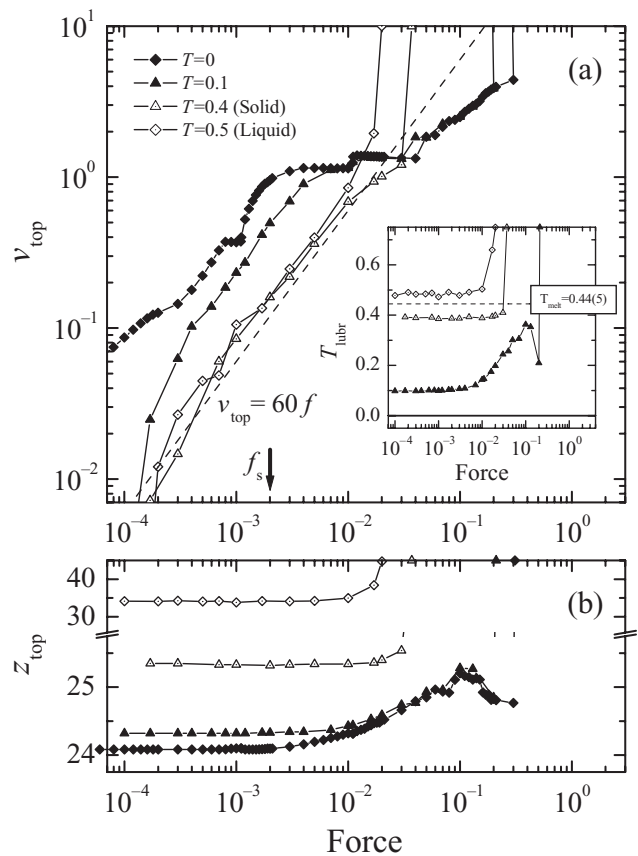


Figure 5. (a) v_{top} versus the dc force f for the flat system at different temperatures when one starts from the perfect-sliding regime. The inset shows the lubricant temperature versus f (the dashed horizontal line corresponds to the melting temperature). (b) Dependence $z_{top}(f)$ at different temperatures.

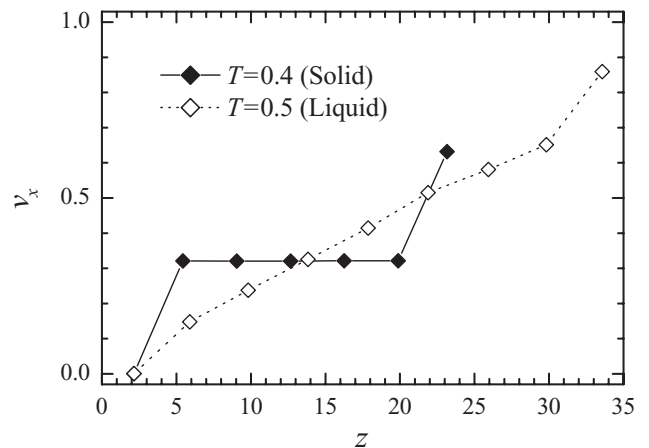


Figure 6. Distribution of x -velocity across the lubricant film for the flat system in the solid ($T = 0.4$, perfect sliding) and liquid ($T = 0.5$, LS) states at the force $f = 0.01$.

2.2.4. Driving through the attached spring. When the driving velocity increases, the $T = 0$ perfect-sliding system demonstrates the following sequence of transitions: stick–slip \rightarrow chaotic (irregular) motion \rightarrow smooth sliding. This scenario remains approximately the same for nonzero temperatures, although the perfect-sliding regime is disturbed due to thermal fluctuations. For example, from figure 8 one can see that the $T = 0$ perfect sliding at the low driving velocity $v_s = 0.1$ changes to thermally activated motion at $T = 0.3$; at

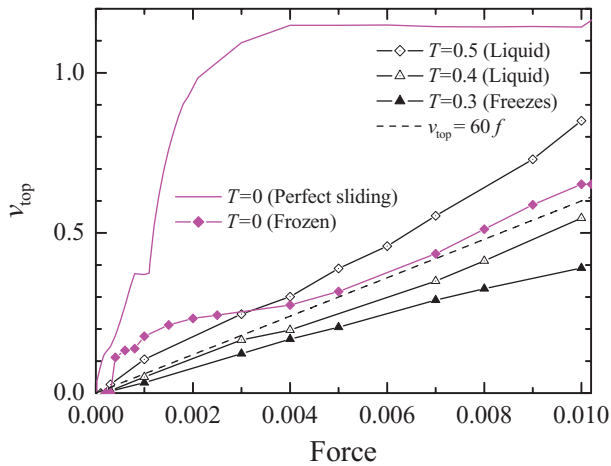


Figure 7. v_{top} versus f for the flat ‘amorphous’ system at different temperatures as indicated in the legend.

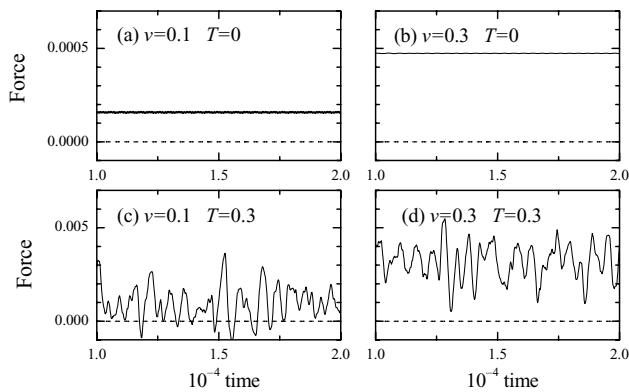


Figure 8. Friction force as a function of time for the flat system obtained with the attached spring algorithm at zero temperature (top row) and at $T = 0.3$ (bottom row).

higher driving velocities the kinetic friction increases with temperature as well. Note also that the kinetic friction force increases with the driving velocity.

If one uses the algorithm with the attached spring for the ‘amorphous’ lubricant, we again observe the transition from stick–slip to smooth sliding, where the lubricant film does not melt during slips. However, as the static friction f_s is much larger for the ‘amorphous’ lubricant than that for the perfect system, the velocity v_c of the transition from stick–slip to smooth sliding should also be larger, provided the relaxation time remains approximately the same. Indeed, in the simulations we observed that $v_c < 0.3$ for the ‘amorphous’ system as compared with $v_c \sim 0.03$ for the perfect lubricant structure. A typical scenario of the transition is shown in figure 9.

During smooth sliding the lubricant is heated; also during stick–slip, the lubricant temperature jump-like increases when the system slips. If these jumps of T are lower than T_{melt} , then the lubricant remains in the initial metastable state. However, if T during a slip approaches T_{melt} or exceeds it, the lubricant may reorder and take the (almost) ideal configuration. After that, the system will behave as it was described above for the crystalline lubricant film (e.g. we observed either the perfect sliding or almost that, with the kinetic friction 2–3 times larger than the perfect-sliding value). Such a sliding-induced

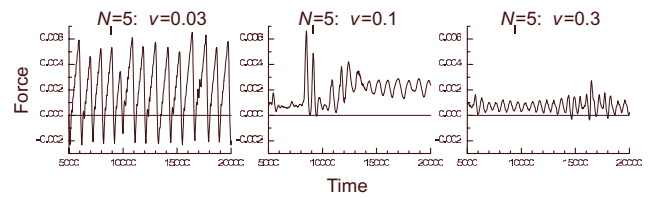


Figure 9. Friction force versus time for three values of the driving velocity (indicated in the legend) for the flat system with ‘amorphous’ lubricant.

ordering (accompanied by squeezing) was observed for all systems (i.e. for $N_l = 2, 3$ and 5) and is described in [3, 16].

Finally, we present the simulation results obtained with the spring algorithm for the case of the curved top substrate. At stick in the stick–slip regime, the lubricant always takes a structure with five layers in the narrow region and six layers in the wide region (figure 3). The lubricant is always ordered due to sliding and moves as a whole together with the top (curved) substrate in the smooth-sliding regime as well as during slips in the stick–slip regime. The values f_s and v_c may differ in different runs but are always relatively low, $f_s \sim 0.02$ and $v_c < 0.3$. The lubricant keeps the crystalline structure during slip as well as at smooth sliding. Thus, for the curved geometry we again observe the (almost) perfect sliding, but now only at the single interface, between the flat substrate and the lubricant.

3. Phenomenology

3.1. The energy balance approach

It is evident that kinetic friction emerges due to energy loss because of the motion of lubricant atoms with respect to the substrates. The kinetic energy of this motion is transferred into the substrates (through excitation of phonons and electron–hole pairs) and finally is dissipated in the substrates being transformed into heat. Therefore, the most natural way to calculate the kinetic friction is through energy balance arguments. Namely, the energy $dE_{\text{in}}/dt = Fv_{\text{top}} = N_{\text{sub}}f v_{\text{top}}$ pumped into the system per time unit due to external driving must be equal to the energy dE_{diss}/dt dissipated in the substrates. We have already used such an approach for the perfect sliding regime at zero temperature and have obtained the ‘universal’ dependence discussed in [3, 5]. This dependence agrees with simulation data for low velocities $v_{\text{top}} \ll 1$; at higher velocities, we had to take into account resonant excitation of phonons in the lubricant film with a number of fitting parameters. In the present work, we extend this approach to nonzero temperatures. However, to avoid the introduction of poorly defined parameters, now we will ignore the resonant excitation of phonons in the lubricant.

The only way of energy dissipation in our model is through the viscous damping term $m_1\eta(z, v)v$ in the equations of motion. Recall that the damping coefficient $\eta(z, v)$ depends on the distance z from the corresponding substrate and on the relative velocity v with respect to it, according to the expression $\eta(z, v) = \eta_1(z)\eta_2(v)$.

When the lubricant has an effective temperature T_{lub} due to heating by the substrate as well as by the

external driving, then its atoms move with a thermal velocity $\langle v_{\text{th}} \rangle = (k_B T_{\text{lub}}/m_1)^{1/2} \sim 0.3\text{--}0.7$ at temperatures $T_{\text{lub}} \sim 0.1\text{--}0.5$ (because the variation of temperature across the lubricant is small according to simulation results, in what follows we assume that all lubricant atoms have the same temperature T_{lub}). When a lubricant atom is near a substrate at a distance z_1 from the nearest surface and moves with an average velocity v_1 with respect to it, then it loses per time unit the energy

$$\epsilon(v_1; T_{\text{lub}}) = m_1 \eta_1(z_1) \int_{-\infty}^{+\infty} dv \eta_2(v) v^2 P(v - v_1; T_{\text{lub}}), \quad (3)$$

where $P(v; T) = (m_1/2\pi k_B T)^{1/2} \exp(-m_1 v^2/2k_B T)$ is the Maxwell distribution. In the thermodynamic equilibrium state, $v_1 = 0$ and $T_{\text{lub}} = T_{\text{sub}}$, this loss must be compensated for by ‘energy gain’ due to the stochastic force in the Langevin equation, which acts on the mobile atoms from the substrate thermostat.

Let N'_{at} be the number of atoms in the lubricant layer just adjoined to the substrate surface, and v_{1x} the average x -velocity of atoms in this (closest to the substrate surface) layer relative the substrate, while $v_{1y} = v_{1z} = 0$ for the motion along y and z . The total energy loss due to friction can be estimated as

$$\frac{dE_{\text{diss}}}{dt} \approx s N'_{\text{at}} E_1(v_{1x}), \quad (4)$$

where

$$E_1(v_{1x}) = \epsilon(v_{1x}; T_{\text{lub}}) + 2\epsilon(0; T_{\text{lub}}) - 3\epsilon(0; T_{\text{sub}}). \quad (5)$$

The first contribution in E_1 comes from the x -motion, and the second one, from the motion along y and z . The last term in (5) describes the energy gain coming from the thermostat to mobile atoms due to the action of the stochastic force; this contribution has to be subtracted from the frictional losses. In the thermodynamic equilibrium state, the energy gain must be equal to the energy loss due to the thermostat, $\epsilon(0; T_{\text{sub}})$. We assume that this contribution (from the stochastic force that emerged due to the thermostat) remains the same in the nonequilibrium driven state. The factor $s = 2$ in front of the rhs of (4) appears in the case of symmetric sliding, where there are two sliding lubricant/substrate interfaces. In the asymmetric case, when there is only one sliding interface, one has to put $s = 1$ and

$$\frac{dE_{\text{diss}}}{dt} \approx N'_{\text{at}} [E_1(v_{1x}) + E_1(0)], \quad (6)$$

where the first contribution comes from the sliding interface and the second one, from the stick lubricant/substrate interface.

From the equality $dE_{\text{in}}/dt = dE_{\text{diss}}/dt$, we finally obtain for the kinetic friction force

$$f_k \approx m_1 G \eta_1(z_1) \mathcal{F}(v_{\text{top}}), \quad (7)$$

where $G \equiv s N'_{\text{at}}/N_{\text{sub}}$ and $\eta_1(z_1)$ are ‘geometrical’ factors which only indirectly depend on the velocity and temperature through a change of the lubricant structure due to sliding (typically $G < 1.2$ and $\eta_1 \sim 0.1$ in our model). The last factor in (7) is the main one that determines the dependence of the

kinetic friction on the driving velocity and temperature, and is defined (for the symmetric sliding, $s = 2$) as

$$\mathcal{F}(v_{\text{top}}) = v_{\text{top}}^{-1} \int_{-\infty}^{+\infty} dv \eta_2(v) v^2 [P(v - v_{1x}; T_{\text{lub}}) + 2P(v; T_{\text{lub}}) - 3P(v; T_{\text{sub}})]. \quad (8)$$

If we take into account only the minimal contribution η_{min} in (2), then the factor \mathcal{F} becomes equal to

$$\mathcal{F}_{\text{min}}(v_{\text{top}}) = \eta_{\text{min}} \left[v_{1x}^2 + \frac{3k_B}{m_1} (T_{\text{lub}} - T_{\text{sub}}) \right] / v_{\text{top}}, \quad (9)$$

which grows linearly with the velocity (at $T_{\text{lub}} = T_{\text{sub}}$) as well as with the lubricant temperature (at fixed v_{top} and T_{sub}).

In the general case, the factor \mathcal{F} also grows with the driving velocity and temperature. Its value is determined by the velocity v_{1x} and the lubricant temperature T_{lub} . It is easy to find v_{1x} in the case of a solid lubricant: $v_{1x} = v_{\text{top}}/2$ for symmetric sliding, while $v_{1x} = v_{\text{top}}$ for asymmetric sliding. In the case of a liquid lubricant (the LS regime), one has $0 < v_{1x} < v_{\text{top}}/2$, as will be discussed in section 3.6. As for the lubricant temperature, its value depends on the sliding velocity due to sliding-induced heating; this question is considered in section 3.3.

3.2. The geometrical factor

While the factor \mathcal{F} in expression (7) increases with the driving velocity and temperature, the geometrical factors G and η_1 decrease, thus compensating the growth. Firstly, the lubricant thickness d increases with the lubricant temperature due to thermal expansion. If one neglects the interaction between the lubricant atoms, then from the ideal-gas equation of state $pV = Nk_B T$, substituting $p = f_{\text{load}}/a_s^2$ for the pressure, $V = Ad = N_{\text{sub}} a_s^2 d$ for the volume ($A = N_{\text{sub}} a_s^2$ is the surface area) and $N = N_1 N_{\text{at}}$ for the total number of lubricant atoms, we obtain $d = d_0 + \beta_{z0} T_{\text{lub}}$ with $\beta_{z0} = N_1 N_{\text{at}} / (N_{\text{sub}} f_{\text{load}})$, or $\beta_{z0} = 30.3$ for the parameters used in the simulations. Let z_s be the coordinate of the surface layer of the substrate ($z_s \approx 2.09$ in the simulation; due to the high hardness of the substrate, we will neglect its thermal expansion in what follows) and \tilde{d} the distance between the surface layers of the top and bottom substrates (see figure 10). Then we have $z_{\text{top}} = \tilde{d} + 2z_s$. Figure 11 demonstrates that the dependence $z_{\text{top}}(T_{\text{lub}})$ for the liquid lubricant can be described by the linear dependence

$$z_{\text{top}} \approx z_{\text{top},0} + \beta_z T_{\text{lub}}, \quad (10)$$

if we put $\beta_z = (6/5)\beta_{z0} \approx 36.4$, i.e. $\tilde{d} = d(N_1 + 1)/N_1$ for the $N_1 = 5$ case. For the solid state of the lubricant, however, the coefficient β_z is much smaller.

Secondly, the geometrical factor G is directly proportional to N'_{at} , i.e. to the number of atoms in the lubricant layer just adjoined to the substrate surface (due to exponential decrease of the factor η_1 with the distance from the substrate, we can neglect contributions from the second and more removed layers). If N'_1 is the effective number of layers in a given configuration, then N'_{at} can be found from the conservation of the total number of atoms, $N'_{\text{at}} N'_1 = N_{\text{at}} N_1$. Evidently, for the perfect crystalline structure

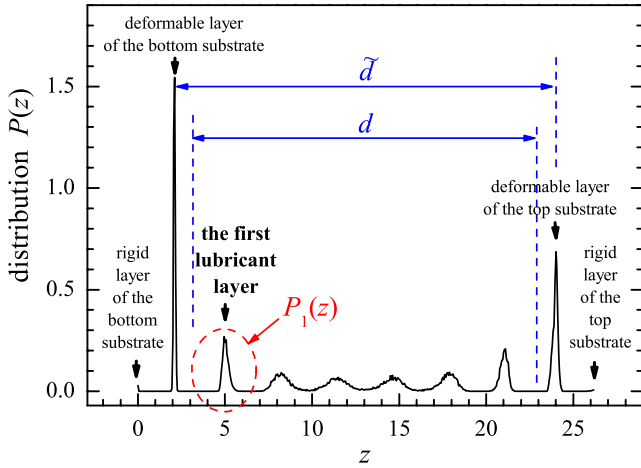


Figure 10. Distribution of atomic concentration across the lubricant in the LS regime (schematically).

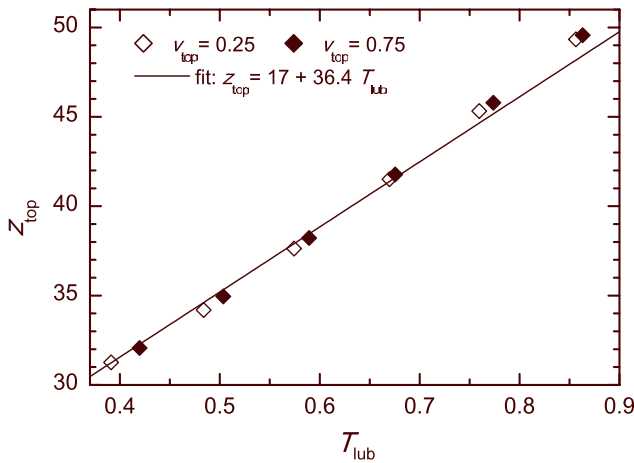


Figure 11. Dependence of the z -position of the top substrate on the temperature of the lubricant film in the LS regime. Symbols show simulation data, whereas the line describes the linear fit (10).

of the lubricant, we have $N'_{\text{at}} = N_{\text{at}}$. From the simulation results, it follows that in the case of a hard lubricant with ‘amorphous’ structure, $N_1 < N'_1 \leq N_1 + 1$ so that $N'_{\text{at}} < N_{\text{at}}$. Thus, for the solid lubricant, we can put $N'_{\text{at}} = \alpha_N N_{\text{at}}$, where $\alpha_N < 1$.

The case of a liquid lubricant, when the lubricant structure is changed with the driving velocity and temperature, is more involved. Because of the conservation of the total number of atoms, $N'_{\text{at}} N'_1 = N_{\text{at}} N_1$, the number of atoms that interact with the substrate, N'_{at} , should decrease when the film thickness grows. Indeed, let r be the average interatomic distance between the lubricant atoms. Then, we have $Nr^3 \propto V = Ad \propto \tilde{d}$, or $r \propto \tilde{d}^{1/3}$ and $N'_{\text{at}} \propto A/r^2 \propto \tilde{d}^{-2/3}$. Using (10), we can put $\tilde{d} \approx \tilde{d}_0(1 + \beta'_N T_{\text{lub}})$, where $\beta'_N = \beta_z/\tilde{d}_0$. Thus, for $T_{\text{lub}} > T_{\text{melt}}$, we come to the dependence

$$N'_{\text{at}} = \alpha_N N_{\text{at}} / [1 + \beta_N (T_{\text{lub}} - T_{\text{melt}})]^{2/3}, \quad (11)$$

where T_{melt} is the melting temperature and $\beta_N \approx \beta'_N$. The geometrical factor G , which is determined by N'_{at} , may strongly decrease with temperature and driving velocity, especially in the LS regime.

To find the value of N'_{at} from simulation data, we calculated the distribution of atomic concentration $P(z)$ as

a function of the coordinate z across the lubricant film, and cut the whole distribution, leaving only the distribution $P_1(z)$ around the peak corresponding to the first lubricant layer (see figure 10). Then, the value N'_{at} can be calculated as $N'_{\text{at}} = C \int dz P_1(z)$ with an appropriate normalization constant, C .

As a result of thermal expansion, the distance of the lubricant atoms from the nearest surface should also increase with temperature, e.g., as

$$z_1 \approx z_{10} + \beta_{z1} T_{\text{lub}}, \quad (12)$$

where $\beta_{z1} \sim \beta'_N$. The increase of z_1 will result in the decrease of the coefficient η_1 according to (1). In the case of the solid lubricant, z_1 can be found as a position of the maximum of the distribution $P_1(z)$. However, such a definition is not accurate, especially for the liquid lubricant. Instead, we determined z_1 by the integral

$$z_{1(\text{eff})} = \int dz z \eta_1(z) P_1(z) / \int dz \eta_1(z) P_1(z). \quad (13)$$

3.3. The lubricant temperature

A very important issue in tribological systems is that the lubricant temperature increases with the driving velocity. This dependence may be described approximately by a power law, e.g. $T_{\text{lub}} \approx T_v(v_{\text{top}})$, where $T_v(v) = \beta_v v^\nu$ with some exponent ν . In macroscopic hydrodynamics, the temperature of a body embedded into a liquid grows with the velocity as $T \propto v^2$, which suggests $\nu = 2$ (see in section V.55 [17]). However, from the simulations, it follows that, at least in the case of $T_{\text{sub}} = 0$ and high enough driving velocities, the lubricant temperature changes approximately linearly with the velocity, so that $\nu \approx 1$.

However, the linear dependence $T_v \propto v_{\text{top}}$ is wrong in the limit $v_{\text{top}} \rightarrow 0$. Indeed, if we put $\nu = 1$, $v_{lx} = 0$ and $T_{\text{sub}} = 0$ in (10), we obtain $\mathcal{F}_{\text{min}} = 3\eta_{\text{min}} k_B T_v / (m_1 v_{\text{top}}) \rightarrow 3\eta_{\text{min}} k_B \beta_v / m_1 \neq 0$, which is wrong. Thus, one has either to involve some interpolation formula, which reduces to the power law with $\nu > 1$ at low v_{top} and to linear dependence at high driving velocities, or to find T_{lub} analytically. Besides, at a nonzero substrate temperature, we should have $T_{\text{lub}} > T_{\text{sub}}$. We found that the simulation data can be well fitted with the help of the interpolation formula

$$T_{\text{lub}} = T_{\text{sub}} + T_v(v_{\text{top}}) \exp[-\kappa T_{\text{sub}} / T_v(v_{\text{top}})], \quad (14)$$

which has the correct behaviour $T_{\text{lub}} \approx T_{\text{sub}}$ in the limits $v_{\text{top}} \rightarrow 0$ or $T_{\text{sub}} \gg T_v(v_{\text{top}})$, and $T_{\text{lub}} \approx T_v(v_{\text{top}}) = \beta_v v_{\text{top}}^\nu$ in the case of $T_v(v_{\text{top}}) \gg T_{\text{sub}}$. However, the fitting parameters ν , β_v and κ in (14) can hardly be found analytically.

On the other hand, the lubricant temperature can be found analytically with the help of energy balance arguments similarly to the approach used above: an energy R_+ pumped into the lubricant (per atom and per time unit) must be equal to the dissipated energy R_- . For a lubricant atom moving with an average velocity v_1 , the rate of energy flux from the atom to the substrate is defined by (3), $R_{\text{as}}(v_1, T_{\text{lub}}) \propto \epsilon(v_1; T_{\text{lub}})$. If $v_1 = 0$ and $T_{\text{lub}} = T_{\text{sub}}$ so that the system is in the thermodynamic equilibrium state, the flux R_{as} must be equal to the opposite flux from the substrate to the lubricant,

$R_{sa}(T_{sub}) \propto \epsilon(0; T_{sub})$, which emerges due to the stochastic force in the Langevin equation. If the system state is out of equilibrium, the net energy flux should be equal to the difference between these two fluxes, $R = R_{as} - R_{sa}$. If we write the flux as $R \propto \epsilon(v_l; T_{lub}) - \epsilon(0; T_{sub}) = [\epsilon(v_l; T_{lub}) - \epsilon(0; T_{lub})] + [\epsilon(0; T_{lub}) - \epsilon(0; T_{sub})]$, then the total flux may be split into two parts, $R = R_v + R_-$, where the first contribution R_v emerges due to nonzero average velocity of the lubricant with respect to the substrate, whereas the second contribution R_- is mainly determined by the temperature gradient. Thus, the energy flux from the lubricant to the substrates, which emerges due to the difference in their temperatures, may be defined as

$$R_- = 6m_1 \int_{-\infty}^{+\infty} dv \eta(z, v) v^2 [P(v, T_{lub}) - P(v, T_{sub})], \quad (15)$$

where $\eta(z, v)$ is the ‘substrate’ damping defined by (1) and (2) and determined by the ‘substrate washboard frequency’ $\omega_{wash} = 2\pi v_{lx}/a_s$, and the factor of $6 = 2 \times 3$ in front of this expression is due to two substrates and three degrees of freedom x, y and z . As the rate R_- is proportional to the difference $\Delta T = T_{lub} - T_{sub}$, an increase in the lubricant temperature has to be proportional to R_+ .

The pumped energy R_+ emerges due to the ‘shaking’ of the lubricant during sliding. This rate can be estimated with the help of linear response theory [18, 19] similar to the approach used in [20]. Let the lubricant be perturbed by an oscillating force of an amplitude f_0 and a frequency ω_0 . When one lubricant layer slides over another with a relative velocity v_0 , it is disturbed with a ‘lubricant washboard frequency’ $\omega_0 = 2\pi v_0/r$, where r is the average interatomic distance in the lubricant. Then, the rate R_+ can be found as

$$R_+ = \frac{\pi s f_0^2}{4m_1} \int_{-\infty}^{+\infty} dv \rho_{lub}(2\pi v/r) [P(v - v_0, T_{lub}) - P(v, T_{lub})], \quad (16)$$

where $\rho_{lub}(\omega)$ is the (local) density of phonon states in the lubricant normalized as $\int_0^\infty d\omega \rho_{lub}(\omega) = 1$.

The value v_0 in (16) is directly proportional to the driving velocity v_{top} , although it has to be defined in different ways for different types of sliding. In the limit $v_{top} \rightarrow 0$, (16) gives $R_+ \propto v_0^2$, which leads to the correct low-velocity relation $\Delta T \propto v_{top}^2$. At higher velocities, the value of R_+ depends on the lubricant phonon spectrum.

The lubricant phonon spectrum is determined by its structure. However, due to the two-dimensionality of the lubricant film, a low-frequency dependence of the density of phonon states must be linear, $\rho_{lub}(\omega) \propto \omega$ at $\omega \rightarrow 0$ (contrary to the law $\rho_{lub}(\omega) \propto \omega^2$ for three-dimensional (3D) systems [19]). As a simple example, let us consider the 2D square lattice with the lattice constant r . It is characterized by the phonon spectrum

$$\omega^2(\mathbf{k}) = \omega_1^2 [\sin^2(rk_x/2) + \sin^2(rk_y/2)], \quad (17)$$

where $\mathbf{k} = (k_x, k_y)$ is the 2D wavevector and ω_1 is determined by the interatomic interaction, $\omega_1^2 = 4g_{11}/m_1$ for the square lattice, where $g_{11} = d^2 V_{11}(r)/dr^2$ is the elastic constant of the lubricant. The spectrum (17) is linear at low frequency,

$\omega(k) \approx 12\omega_1 r k$ at $k \rightarrow 0$. The maximum (Debye) lubricant frequency is equal to $\omega_{max} = \omega_1 \sqrt{2}$. The local density of phonon states for the 2D spectrum (17) can be found analytically [19]:

$$\rho_{lub}(\omega) = \frac{4|\omega|}{\pi^2 \omega_1^2} \mathbf{K} \left(\frac{|\omega| \sqrt{2\omega_1^2 - \omega^2}}{\omega_1^2} \right), \quad (18)$$

where $\mathbf{K}(x)$ is the complete elliptic integral of the first kind. The density (18) is linear at low frequency, $\rho_{lub}(\omega) \approx 2\omega/\pi\omega_1^2$ at $\omega \rightarrow 0$, and has a logarithmic singularity in the middle of the phonon zone at $\omega = \omega_1$, where $\rho_{lub}(\omega) \approx \ln(\omega_1/\omega - \omega_1)$.

In the case of a liquid lubricant, one may use a ‘gas spectrum’

$$\rho_{lub}(\omega) = \frac{2|\omega|}{\pi\omega_1^2} \exp\left(-\frac{\omega^2}{\pi\omega_1^2}\right), \quad (19)$$

and the rate R_+ can be found analytically.

We emphasize that all the expressions presented above are valid for the smooth sliding regime only, i.e. for the driving velocities $v_{top} > v_c \sim 0.1$. In the stick–slip regime, the system dynamics is governed by the static friction force f_s . The same comment is true for creep motion at low driving at $T_{sub} > 0$, when the motion is thermally activated and is governed by a factor $\exp(-a' f_s/k_B T_{sub})$, where a' is some length parameter of the order of the lattice constant.

In what follows, we apply the described phenomenological approach to the $N_1 = 5$ hard-lubricant system to explain the simulation data of section 2.

3.4. The perfect sliding

More simple is the case when the lubricant remains in the solid state during sliding and its structure does not change with time. For the perfect sliding, we take $v_{lx} = v_{top}/2$, $s = 2$ and $N'_{at} = N_{at}$ so that $G = 2N_{at}/N_{sub} = 1.212$. From the simulation data presented in figure 5, we extracted other parameters: $z_{top,0} \approx 23.95$, $\beta_z \approx 3.6$, $z_{10} \approx 5.21$, $\beta_{z1} \approx 0.3$ and $z_s \approx 2.12$. The phenomenological dependences obtained with these parameters and with the value $f_0 = 0.2$ for the only fitting parameter are presented in figure 12. One can see a rather good qualitative and even quantitative agreement with the simulation data of figure 5 (at high driving velocities, $v_{top} > 1$, the friction force observed in the simulations is higher than that of the phenomenological approach, because the latter ignores all resonances inside the lubricant). Note that if we ignore all temperature dependences, we obtain in the $T_{sub} = 0$ case the ‘universal’ dependence introduced in [5].

3.5. The solid lubricant with the ‘amorphous’ structure

In the case of ‘amorphous’ lubricant, we found in the simulations that $N'_1 \approx N_1 + 1$ so that $N'_{at} = N_{at} N_1/N'_1$ or $\alpha_N = 5/6 \approx 0.833$ (simulation suggests that the value $\alpha_N \approx 0.81$; note that this parameter depends on a particular metastable configuration). From the simulation data of figure 2, we extracted other parameters: $z_{top,0} \approx 26.78$, $\beta_z \approx 2.33$, $z_{10} \approx 5.22$, $\beta_{z1} \approx 0.333$ and $z_s \approx 2.112$. The phenomenological dependences obtained with these parameters for the case of

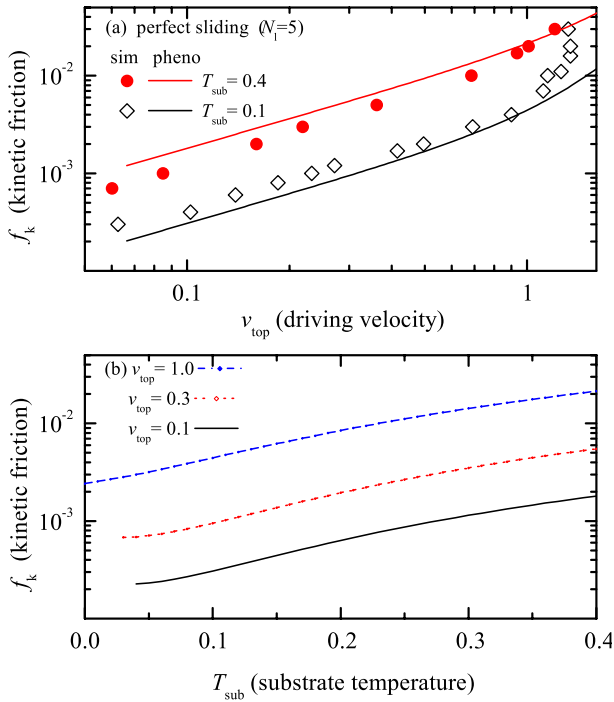


Figure 12. Phenomenological dependences for the perfect sliding of the $N_l = 5$ solid lubricant for $f_0 = 0.2$. (a) Dependence of the kinetic friction force on the sliding velocity at $T_{sub} = 0.1$ (open diamonds) and $T_{sub} = 0.4$ (red solid circles). The symbols correspond to simulation data of figure 5. (b) Dependence of the kinetic friction on the substrate temperature for three values of the sliding velocity, $v_{top} = 0.1, 0.3$ and 1.

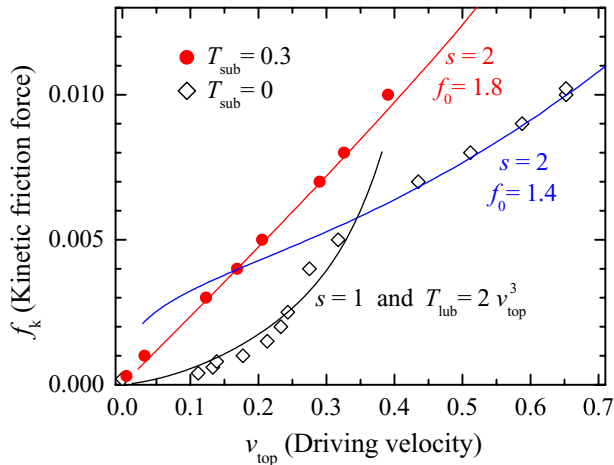


Figure 13. Phenomenological dependences of the kinetic friction force on the sliding velocity at $T_{sub} = 0$ (blue curve and open diamonds, the symbols correspond to simulation data of figure 2) and $T_{sub} = 0.3$ (red curve and solid circles) for the ‘amorphous’ lubricant.

symmetric sliding ($s = 2$) are presented in figure 13 (also we took into account a small heating of the mobile substrate layers with the help of a dependence $T_{sub1} \approx 0.0017v_{top}^2$). Note, however, that we had to take different values for the fitting parameter f_0 ; namely, we used $f_0 = 1.4$ for the $T_{sub} = 0$ case, but $f_0 = 1.8$ for $T_{sub} = 0.3$.

According to the $T = 0$ simulation, the sliding becomes asymmetric ($s = 1$) at low driving velocities $v_{top} < 0.3$. This is reasonable, because the system configuration is not symmetric now, so that the sliding may take place at one

of the lubricant/substrate interfaces only. In this case, we put $v_{lx} = v_{top}$. Unfortunately, we were unable to obtain good quantitative agreement with simulation data with the help of the procedure described above, although we obtained the correct order of magnitude of the friction force. Instead, good agreement was achieved with the help of an artificial dependence $T_{lub} \approx 2 v_{top}^3$, as shown in figure 13 by the black curve.

One may think that the ‘amorphous’ lubricant may lead to a smaller friction than the crystalline one, because the geometrical factor is smaller in the former case. However, we have to take into account the following factors: (i) in the case of the ‘amorphous’ lubricant, the load is distributed over fewer atoms, N'_{at} . Therefore, the value of z_1 is smaller and the factor η_1 is larger than those for the crystalline lubricant. (ii) The truly incommensurability of the lubricant/substrate interface is destroyed in the ‘amorphous’ case. Both the factors (i) and (ii) increase the sliding-induced heating of the lubricant and therefore the friction. (iii) When the sliding is asymmetric at low driving, there is only one sliding interface. Therefore, the value of v_{lx} is two times larger in this case. As the rate of energy transfer from a moving lubricant atom into the substrate, which is determined by the coefficient $\eta(z, v)$, strongly increases with the relative velocity according to (2), this leads to higher friction as well.

Note that in the case when the lubricant is solid (either crystalline or ‘amorphous’), the kinetic friction increases with temperature and/or velocity in the smooth sliding regime. However, for the creep motion, the dependence is opposite, i.e. the sliding velocity increases with temperature at a constant driving force, because creep is a thermally activated process.

3.6. The LS regime

Finally, let us consider the liquid lubricant case. When the confined film is molten, its thickness changes with the temperature and driving velocity. In this case, the geometrical factor G , which is proportional to N'_{at} determined by (11), will strongly decrease with temperature, and this effect may compensate or even overcome the increase of kinetic friction owing to the factor \mathcal{F} .

It is easy to extract from simulations the parameters $\beta_z \approx 36.4$, $z_{top,0} \approx 17$ (see figure 11) and $z_s \approx 2.09$; that gives $\beta'_N \approx 2.84$. To find N'_{at} , we calculated the distribution of atomic concentration around the first lubricant layer $P_1(z)$ (see figure 10) and then integrated it, $N'_{at} = C \int dz P_1(z)$. The result of this analysis is shown in figure 14. One can see that the dependence $N'_{at}(T_{lub})$ can be fitted with a good accuracy by the dependence (11) with $T_{melt} = 0.44$, $\beta_N = \beta'_N$ and $\alpha_N = 0.65$.

Next, we have to know the position z_1 of the first lubricant layer with respect to the substrate, because it determines the exponential factor η_1 in (1). We calculated it with the help of (13); this leads to the dependence (12) with $z_{10} = 5.41$ and $\beta_{z1} \approx 0.313$ as demonstrated in figure 15.

Then, we have to know the average velocity v_{lx} of the first lubricant layer with respect to the substrate. Using the distribution of x -velocities across the lubricant obtained in simulation (figure 6), we schematized it as shown in figure 16.

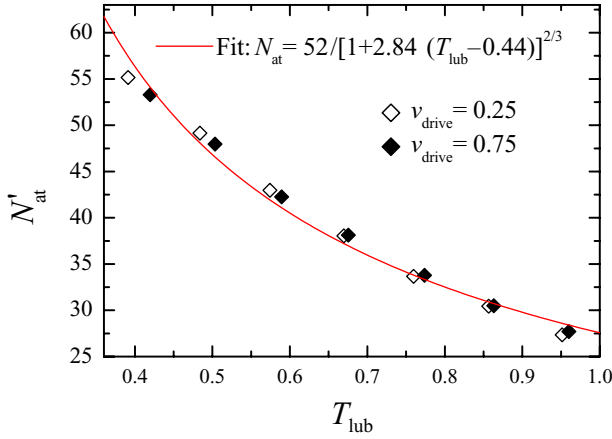


Figure 14. Dependence of N'_{at} on the lubricant temperature extracted from simulation data for the LS regime. The curve shows the dependence (11) with $T_{\text{melt}} = 0.44$, $\beta_N = 2.84$ and $\alpha_N = 0.65$.

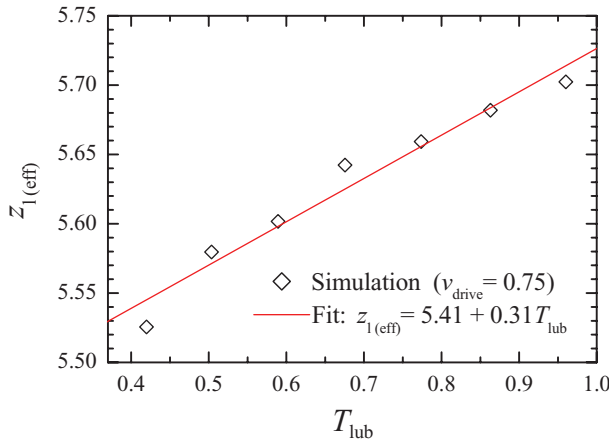


Figure 15. Dependence of the average coordinate of the first lubricant layer $z_{1(\text{eff})}$ on the lubricant temperature extracted from simulation data for the LS. The line corresponds to the linear fit $z_{1(\text{eff})} = 5.41 + 0.31 T_{\text{lub}}$.

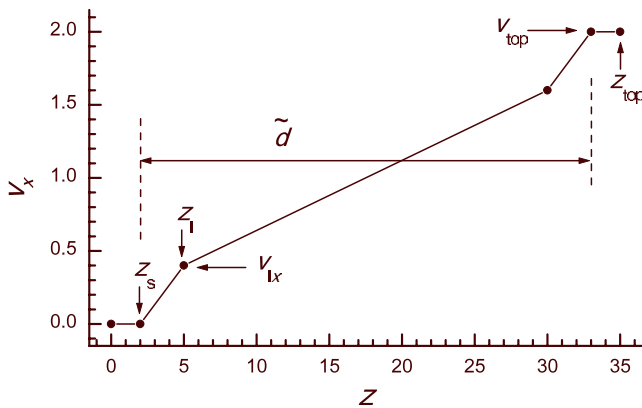


Figure 16. Schematic presentation of the distribution of the x -velocity of lubricant atoms across the lubricant.

The dependence $v_x(z)$ is linear within the lubricant, but undergoes jumps at the substrate/lubricant interfaces. Using this picture, we assume that v_{lx} can be described by the expression

$$v_{lx} = \alpha v_{\text{top}}(z_1 - z_s)/\tilde{d}, \quad (20)$$

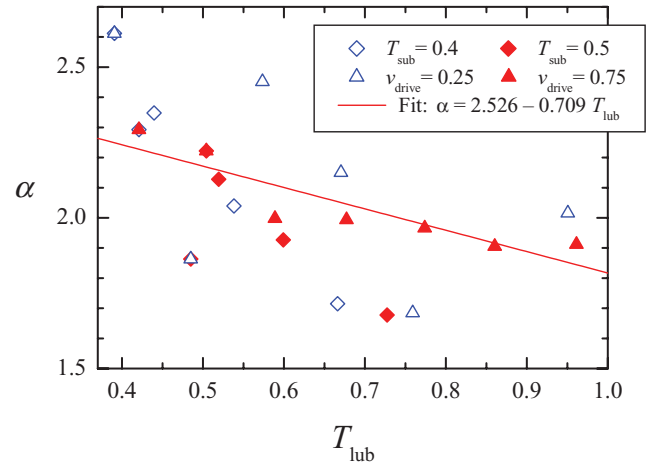


Figure 17. Dependence of the parameter α in (20) on the lubricant temperature. The line corresponds to the linear fit $\alpha = 2.53 - 0.71 T_{\text{lub}}$.

which includes a phenomenological parameter, α . The values of α extracted from the simulation data are presented in figure 17. A linear fit of these data gives the dependence $\alpha = 2.53 - 0.71 T_{\text{lub}}$.

Finally, the increase in lubricant temperature due to sliding was calculated by the method described in section 3.3 with the only fitting parameter f_0 ; this gives the value $f_0 \approx 4.6$ if we use the ‘gas’ spectrum of the lubricant film, (19) (also we took into account a small increase in temperature of the surface (mobile) layer of the substrate with the help of (14) with the fitting parameters $\nu \approx 1$, $\kappa \approx 0.1$ and $\beta_\nu \approx 0.026$). Combining all things together, we obtained the phenomenological dependences presented in figure 18. As seen, the phenomenological approach leads to a rather good qualitative and even quantitative description of the dependences observed in simulation. Note that now the kinetic friction decreases when the substrate temperature grows, contrary to the behaviour observed for the solid lubricant.

4. Discussion and conclusion

The simulation results of section 2.2 may be summarized as follows. When the interaction within the lubricant is stronger than the lubricant–substrate interaction, then the film remains in the solid state at smooth sliding or during slips for stick–slip motion, provided the substrate temperature is not too large. The melting temperature of the confined film is so high that it cannot be reached only because of heating of the lubricant due to sliding. The sliding always occurs at the lubricant/substrate interfaces, where the bonds are weaker.

In the case when the lubricant is crystalline without defects and is in contact with the atomically smooth flat substrate surfaces, both static and kinetic friction forces are very small. This is just the ideal case of negligible friction predicted for the contact of two incommensurate solid surfaces. The static force f_s depends linearly on the load according to Amonton’s law $f_s = f_{s0} + \alpha_s f_{\text{load}}$, but the proportionality coefficient is extremely small, $\alpha_s \sim 10^{-3}$ or even smaller [3]. Moreover, f_s does not change with the time of stationary contact. Due to so small values of f_s , the transition from stick–slip to smooth sliding also occurs at a

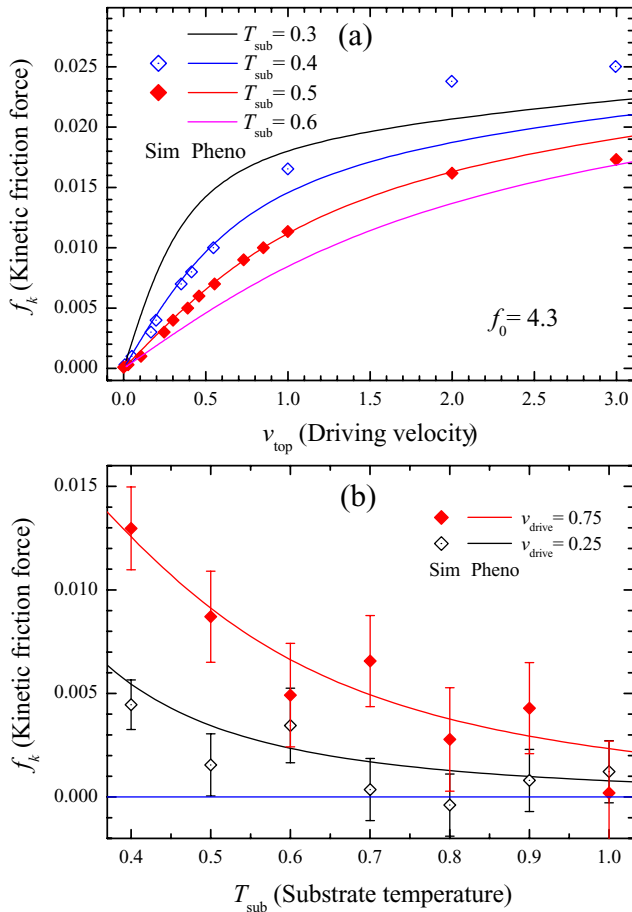


Figure 18. Dependence of the kinetic friction force on the driving velocity at a fixed substrate temperature (a) and on the substrate temperature at a fixed driving velocity (b) for the LS regime. Symbols correspond to simulation data, while solid curves describe the phenomenological dependences.

rather low velocity, $v_c \sim 0.03$. The kinetic friction force in the perfect-sliding regime is very small too, $f_k \sim 10^{-4} - 10^{-3}$ (so that $\mu_k \equiv f_k/f_{load} \sim 10^{-3} - 10^{-2}$), but it strongly increases with the sliding velocity.

When the lubricant is annealed and then frozen in a metastable ('amorphous') state, the friction depends on the particular metastable configuration. The static friction force takes values of order $f_s < 0.1$ and follows Amontons' law with $\alpha_s \sim 0.3$. The transition from stick-slip to smooth sliding takes place at $v_c \sim 0.1 - 0.5$ (this value depends on the particular configuration that the film had in the stick state). During the slip, the kinetic friction force also depends on the 'starting' configuration, and may change during sliding due to reordering within the film. At low velocities, the sliding is asymmetric, the lubricant sticks to either the bottom or the top substrate. The kinetic friction force increases with the driving velocity as $f_k \approx B v_{top}$ ($B \approx 0.015$ for the flat geometry, and $B \approx 0.025$ for the curved one). At the onset of slip, the lubricant temperature increases and may exceed the melting temperature. In this case, the film is ordered and may even take the ideal crystalline configuration, so that the perfect-sliding mechanism will operate further.

If the lubricant is in the molten state, the kinetic friction force takes intermediate values and depends on the driving velocity as $f_k \approx 0.017 v_{top}$.

In all cases, the friction depends on the substrate temperature. If one starts from the perfect-sliding state, then the velocity decreases when T grows (for the constant-force algorithm) until the film melts. The same is true for the case of 'amorphous' lubricant, although the mobility in this case is much lower. After the melting, the mobility grows with temperature, although it remains lower than the $T = 0$ perfect-sliding value. Thus, for the solid state of the lubricant, the friction increases with the substrate temperature, while for the liquid lubricant, the dependence is opposite: the friction decreases when T grows. Note, however, that such a behaviour corresponds to the smooth sliding regime. For the creep motion, which corresponds to the thermally activated process, the friction should decrease when temperature grows.

Note also that in all cases the friction increases with the driving velocity. Such a dependence is in agreement with general physical reasons, because, otherwise, the steady motion will be unstable.

The simulation results can be satisfactorily explained with the help of the phenomenological theory presented in section 3. Almost all phenomenological parameters that we extracted from simulation data may in principle be calculated from first principles or estimated at least, except the two fitting parameters f_0 and α . The first parameter, the coefficient f_0 in (16), describes the amplitude of the oscillating ('shaking') force responsible for the sliding-induced heating of the lubricant. Note that for the solid state of the lubricant film, the value of the fitting parameter f_0 correlates with the value of the static friction f_s : the smallest value ($f_0 = 0.2$) was found for the perfect sliding regime, whereas much larger values ($f_0 = 1.4 - 1.8$), for the 'amorphous' lubricant structure. The largest value ($f_0 = 4.6$) was obtained for the liquid lubricant. We could suggest that the value of f_0 is proportional to 'defectivity' of the lubricant film structure, although we have no clear understanding of this problem, and it requires further investigation.

Secondly, the friction force in the LS regime strongly depends on the velocity of the first lubricant layer relatively to the substrate. According to (20), v_{lx} is determined by the parameter α , i.e. by the gradient of x -velocity at the substrate/lubricant interface. This question is closely related to the 'slip' or 'no-slip' behaviour of a liquid flow near a solid surface. The latter is characterized by the so-called slip length, defined as

$$L_s \equiv v_{lx} \left/ \frac{dv_x}{dz} \right|_{z=z_1} = \frac{v_{lx} (\tilde{d} - 2z_1)}{(v_{top} - 2v_l)}$$

or

$$L_s = \alpha \frac{(z_1 - z_s) (\tilde{d} - 2z_1)}{[\tilde{d} - 2\alpha (z_1 - z_s)]}.$$

In turn, the slip length is determined by the liquid-surface interaction, i.e. either the surfaces are wetting or non-wetting by the lubricant [21] (the latter situation corresponds to the hard-lubricant system studied in this work). Recently, the problem of slip length was studied with the help of the variable-density Frenkel-Kontorova model [22]. It was predicted that the slip length at low driving is proportional to the square root of the elastic constant of the liquid, or

$\alpha \propto V_{\parallel}^{1/2}$ in our model, which is in qualitative agreement with the simulation results [3].

Although the phenomenological theory presented above still uses some parameters, it allows us to explain the simulation results. In particular, it naturally explains the increase of kinetic friction with the driving velocity. Then, it explains the temperature dependence of the friction, which emerges due to the interplay of two factors, \mathcal{F} and $G\eta_1$, in (7): the first factor increases with temperature, whereas the geometrical one, $G\eta_1$, decreases with T . Thus, the phenomenological theory allows us to predict, at least qualitatively, the behaviour of other tribological systems in a general framework.

Finally, note that the steady-state regimes considered in the present work correspond to relatively high velocities, $v > 0.03$ in our dimensionless units, or $v > 10 \text{ m s}^{-1}$. At lower velocities the microscopic motion always corresponds to stick–slip in the case of planar geometry of the interface [20], although it may look like ‘smooth’ on a macroscopic scale.

Acknowledgments

We wish to express our gratitude to B N J Persson, M Paliy and T Dauxois for helpful discussions. This research was supported in part by the EU Exchange Grant within the ESF programme ‘Nanotribology’ (NANOTRIBO) and the Cariplo Foundation (the Landau Network—Centro Volta).

References

- [1] Persson B N J 1998 *Sliding Friction: Physical Principles and Applications* (Berlin: Springer-Verlag)
- [2] Robbins M O and Muser M H 2000 Computer simulation of friction, lubrication and wear *Handbook of Modern Tribology* ed Bhushan B (Boca Raton, FL: CRC Press)
- [3] Braun O M and Naumovets A G 2006 *Surf. Sci. Rep.* **60** 79
- [4] Thompson P A and Robbins M O 1990 *Phys. Rev. A* **41** 6830
Thompson P A and Robbins M O 1990 *Science* **250** 792
Robbins M O and Thompson P A 1991 *Science* **253** 916
- [5] Braun O M and Peyrard M 2001 *Phys. Rev. E* **63** 046110
- [6] Hirano M and Shinjo K 1990 *Phys. Rev. B* **41** 11837
Hirano M, Shinjo K, Kaneko R and Murata Y 1997 *Phys. Rev. Lett.* **78** 1448
- [7] Dienwiebel M, Verhoeven G S, Pradeep N, Frenken J W M, Heimberg J A and Zandbergen H W 2004 *Phys. Rev. Lett.* **92** 126101
- [8] Muser M H and Robbins M O 2000 *Phys. Rev. B* **61** 2335
- [9] Thompson P A, Robbins M O and Grest G S 1995 *Israel J. Chem.* **35** 93
- [10] He G and Robbins M O 2001 *Tribol. Lett.* **10** 7
He G and Robbins M O 2001 *Phys. Rev. B* **64** 35413
- [11] Gardiner C W 1983 *Handbook of Stochastic Methods* (Berlin: Springer)
- [12] Braun O M and Ferrando R 2002 *Phys. Rev. E* **65** 061107
- [13] Persson B N J and Ballone P 2000 *J. Chem. Phys.* **112** 9524
- [14] Braun O M and Peyrard M 2003 *Phys. Rev. E* **68** 011506
- [15] Valadon Ph 2000 *RasTop: Molecular Visualization Software* online at <http://www.geneinfinity.org/rastop/>
- [16] Braun O M, Paliy M and Consta S 2004 *Phys. Rev. Lett.* **92** 256103
- [17] Landau L D and Lifshitz E M 1987 *Fluid Mechanics* (New York: Pergamon)
- [18] Landau L D and Lifshitz E M 1958 *Statistical Physics* (London: Pergamon)
- [19] Kosevich A M 1988 *Theory of Crystal Lattice* (Vuscha Schkola: Kharkov) (in Russian)
Kosevich A M 1999 *The Crystal Lattice: Phonons, Solitons, Dislocations* (Berlin: Wiley-VCH)
- [20] Braun O M, Peyrard M, Bortolani V, Franchini A and Vanossi A 2005 *Phys. Rev. E* **72** 056116
- [21] Barrat J-L and Bocquet L 1999 *Phys. Rev. Lett.* **82** 4671
- [22] Lichter S, Roxin A and Mandre S 2004 *Phys. Rev. Lett.* **93** 086001